Effect of Wing Plates on Vertical Load Capacity of a Multiline Ring Anchor System in Clay

Junho Lee, S.M.ASCE[1], Charles P. Aubeny, Ph.D., P.E., F.ASCE[2], Sanjay Arwade, Ph.D.[3], Don DeGroot, Sc.D., P.E., M.ASCE[4], Alejandro Martinez, Ph.D., A.M. ASCE[5], and Ryan Beemer, Ph.D., A.M.ASCE[6]

[1]Ph.D. Candidate, Zachry Department of Civil and Environmental Engineering, Texas A&M University, College Station, TX 77843; e-mail: juno918@tamu.edu
[2]Professor, Zachry Department of Civil and Environmental Engineering, Texas A&M University, College Station, TX 77843; e-mail: caubeny@civil.tamu.edu
[3]Professor, Civil and Environmental Engineering, University of Massachusetts Amherst, Amherst, MA 01003; e-mail: arwade@umass.edu
[4]Professor, Civil and Environmental Engineering, University of Massachusetts Amherst, Amherst, MA 01003; e-mail: degroot@umass.edu
[5]Assistant Professor, Civil and Environmental Engineering, University of California, Davis, CA 95616; e-mail: amart@ucdavis.edu
[6]Assistant Professor, Civil and Environmental Engineering, University of Massachusetts Dartmouth, Dartmouth, MA 02747; e-mail: rbeemer@umassd.edu

ABSTRACT

Development of offshore wind in deeper waters that are beyond the feasible range of fixed towers requires a cost-effective anchorage for floating offshore wind turbines (FOWTs). The multiline ring anchor (MRA) system has been devised as a cost-effective anchor for FOWTs, by virtue of its high efficiency, its capability for securing multiple mooring lines, and its adaptability to a wide range of seabed conditions. Taut mooring systems become increasingly attractive as water depth increases, leading to combined horizontal-vertical loading on the anchor. Since the MRA is deeply embedded in the seabed, it has capabilities for resisting the vertical component of the forces imposed by taut moorings. Since the MRA lacks the reverse end bearing resistance of a conventional suction anchor, its design requires careful attention to ensure that it can resist the vertical load demand from a taut mooring. Previous preliminary studies show that the uplift resistance of the MRA in soft clay can be improved by attaching wing plates, increasing anchor size, or installing in deeper depth, the latter being limited by the constraints of suction installation. Wing plates turn out to be a very promising option, but more reliable studies of their performance are needed to support an optimally designed, cost-effective anchor. Thus, rigorous three-dimensional finite element analyses were conducted to understand how wing plates improve the uplift resistance and provide reliable evaluations of the vertical load capacity

of the MRA. The results show that the soil-anchor adhesion factor, the total number of wing plates, and the width of wing plates are important factors contributing to anchor uplift resistance. To investigate an optimal design of the wing plates, a comparative study was carried out to compare the effects of wing plates on minimizing capital costs. The studies show that attaching wing plates can be an economical solution for improving axial capacity.

INTRODUCTION

Offshore renewable resources can have significant advantages over land-based renewable energy due to proximity to coastal population centers, greater consistency and stability, and aesthetic issues (Barter et al. 2020; Musial et al. 2016). With a major portion of offshore wind occurring in deeper water (greater than 60 m), future development of the offshore wind industry trend is expected to shift from fixed to floating offshore wind turbines (FOWTs). However, foundation costs for floating structures increases for FOWTs installed farther offshore and in deeper water (Harris and Grace 2015). The multiline ring anchor (MRA) has been devised as one measure for reducing these costs. The MRA is a ring-shaped anchor designed to be deeply embedded in offshore soils to secure multiple floating platforms (Aubeny et al. 2020, Figures 1 and 2). Attractive features of the MRA include its ability to attach multiple mooring lines to a single anchor, its compact size, its installability in a wide range of soil, applicability to various loading conditions and fewer anchors, and its resilience under unintended loading conditions. Its compactness not only reduces material costs but also permits the use of smaller transport vessels and handling equipment, which is critical to reducing capital costs of large-scale offshore wind energy projects (Diaz et al. 2016; Lee and Aubeny 2020; Lee et al. 2020).

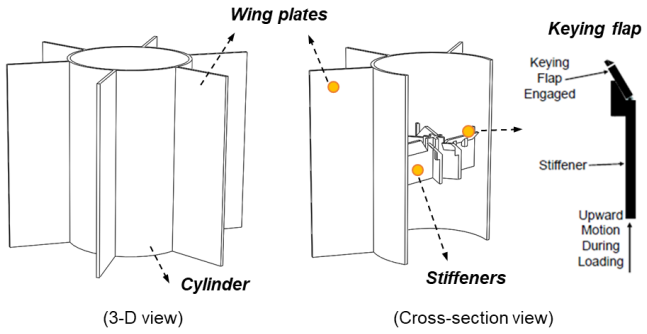

Figure 1. Six-wings MRA and strategies for enhancing load capacity

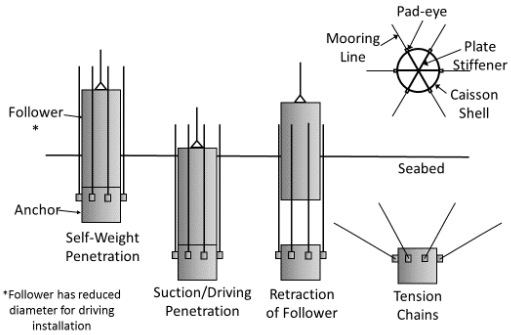

Figure 2. The installation procedure of the MRA (Lee and Aubeny 2020)

Although the MRA is envisioned to be suitable to a wide range of loading and soil conditions, this study solely addresses the vertical load capacity in a soft clay soil profile, with a specific focus on the effectiveness of wing plates. Previous studies that achieving a realistic FOWT spacing in deeper waters dictates the use of taut mooring systems (IEA 2019, Lee et al. 2021). The vertical load demand from taut mooring systems is a primary motivation for the

present study investigating the vertical load capacity of the MRA. Preliminary findings from the study on uplift resistance to extreme conditions showed the axial capacity of the MRA could be increased by various means, such as adding wing plates, increasing the diameter of the tube, and installing stiffeners. However, the axial performance generated by wing plates requires further investigation. Thus, this study focuses on understanding the impacts of wing plates on the vertical capacity of the MRA in clay.

KEY ISSUES FOR WING PLATES ON MRA

Uplift resistance of the MRA in clay. The open-tube configuration of the MRA precludes the development of significant reverse end bearing resistance, and its shorter length reduces the amount of side resistance that can be mobilized relative to a conventional suction caisson (Lee and Aubeny 2021). These effects can be partially offset by side frictional resistance along the inner cylindrical surface of the MRA. However, the uplift resistance of the MRA must still be improved through other means to achieve the comparable capacity to the caisson having the same diameter. Lee et al. (2021) show that the uplift resistance can be enhanced by increasing the diameter of the anchor, attaching wing plates, installing stiffeners, or introduction keying flaps on the stiffeners. The current study focuses on understanding the effects of what was found to be a particularly promising measure, wing plates.

A semi-empirical approach can be instrumental in estimating the effects of wing plates on the axial capacity of the MRA in clay and validating its finite element studies by comparison. Since the MRA consists of a cylindrical core, optional wing plates, and stiffeners (Figure 1), the uplift resistance of the composite cylinder-plate geometry is computed by summing each load capacity component, for which relatively simple equations exist to evaluate the axial capacity. Table 1 summarizes the main premises and the equations for the uplift resistance of the individual elements. While the uplift resistance of the MRA is the summation of each element, this study focuses on the vertical load capacity generated by an opened tube and wing plates to understand how wing plates impact the uplift resistance of the anchor.

Table 1. Sources of uplift resistance for the MRA

Components	Equations	Assumptions	Sources
Ring	$V_{ring} = 2\pi D s_{u\_MRA}(\alpha L + N_c t_{ring})$	Annular tip resistance factor, $N_c = 9$	Andersen et al (2005)
Wing plates	$V_{wing} = 2N_w W_w s_{u_{MRA}}(\alpha L_w + N_e t_{wing} + \alpha t_{wing} L_w / 2W_w)$	End bearing factor, $N_e = 7.5$	Murff et al. (2005)
Stiffeners	$V_{stf} = 2N_{stf} D s_{u\_stf}(\alpha L_{stf} + N_e t_{stf})$	End bearing factor, $N_e = 7.5$	Murff et al. (2005)

where D= the diameter of the cylindrical ring, s_{u_MRA}= the average of the undrained shear strength for the MRA, s_{u_stf}= the average of the undrained shear strength for the stiffeners, α = the adhesion factor between anchor and soil, L=L_w= length of ring and wing plates, and t_{ring}=t_{wing}=t_{stf}= the thickness of the ring, wing plates, and stiffeners.

Considerations for the effect of wing plates on the axial Capacity. Preliminary findings from two-dimensional finite element (2-D FE) studies and plastic limit analysis (PLA) on the effects of wing plates show that the wing plates are effective means to improve the lateral capacity. Additionally, the failure mechanisms and lateral bearing factors vary depending on the width of wing plates W_w, the number of wings N_w, and load angles θ_a (Lee and Aubeny 2021). On the other hand, in view of improving the axial capacity of the MRA, the wing plates simply increase more surface that includes additional side frictional ($=N_w(2W_wL_w+t_{wing}L_w)$) and end bearing areas ($=2N_wt_{wing}W_w$). Thus, the effects of the wing plates are best represented in terms of a wing plate parameter, N_wW_w/R, as relevant to the total area matter, where R is the radius of the cylindrical core. This simplified parameter can provide valuable insights to optimize the MRA design.

Since the undrained shear strength of a typical normally consolidated clay profile increases roughly linearly with the depth, the axial load capacity of the anchor increases similarly. This means that embedding the MRA as deeply as possible is an effective means to increase uplift capacity. On the other hand, the installation techniques such as suction installation may be limited to a certain embedment depth (i.e., penetration to $h/D = 6$, where h = tip embedment depth of the MRA). Thus, increasing the MRA surface area as much as possible is an effective means of enhancing the uplift resistance without having to embed the anchor more deeply. Attaching wing plates is one simple approach to improving the uplift resistance by increasing the surface area. For example, a larger diameter MRA without wing plates can be replaced by a smaller diameter MRA with wings that achieve the same axial capacity. In view of enhancing the uplift resistance, increasing the diameter seems effective as attaching wing plates. However, the wing plates can benefit in substantially reducing transport and installation costs. Since suction installation time is proportional to the inner volume of the cylinder, a larger volume caused by a larger diameter requires a longer time for pumping the water out. Additionally, as the dimensions of the cylindrical core section of the MRA govern the required deck space on a transport vessel, a smaller diameter MRA can be fit onto the vessel for loading more anchors. Therefore, this study investigates the effects of wing plates and optimizes the MRA design in cost-effectiveness.

FINITE ELEMENT STUDIES

The finite element (FE) soil model uses a linearly elastic-perfectly plastic behavior beneath a Tresca yield surface and an associated flow rule. To approximate the undrained loading, the current study assumes a Poisson's ratio, with μ set to 0.49. Since the focus of this study is the characterization of axial bearing factors caused by wing plate parameters, all FE studies took a uniform undrained shear strength (s_u = 1 kPa) and Young's modulus E/s_u = 1,000, which does not affect the ultimate load capacity of the anchor (Chen 1975). The 2-D FE study provides useful insights into the effects of wing plate parameters on the lateral capacity. However, as noted earlier, the increase of uplift resistance is primarily caused by the increase in total area

from wing plates. This requires three-dimensional FE analyses to investigate the influence of wing plates on the axial capacity of the MRA.

The dimensions of the MRA are shown in Figure 1, a 2.8-m diameter by a 4.2-m length of the cylindrical core with wing plate width varying 0.7-1.4m. The MRA was considered as a rigid body, and the soil was modeled using first-order and fully integrated elements (eight-node element). The boundary was positioned 15 diameters of caisson 15*D* away from the MRA. The far-field was modeled using eight-node one-way infinite elements. Since preliminary FE calculations display the convergence of collapse load when the tip embedment depth ratio is greater than h/D = 3, this study considered $h/D = 4$ to simulate the deeply embedded condition. In this study, fine-meshed elements, less than about one-eleventh of the caisson radius, were chosen to achieve a sufficient balance between accuracy and computational efficiency (Figure 3). The 3-D FE model was validated through comparison to the semi-empirical approach for the axial capacity and the exact solution for the lateral capacity (Randolph and Houlsby 1984). The FE computations were about 15% greater than the semi-empirical solution or the exact solution, and the results display acceptable because of the following reasons. Firstly, preliminary findings from rigorous 3-D FE on effects of the aspect ratio of the pile indicate that bearing factor differences between 3-D FE and solutions increase with decreasing aspect ratio (Aubeny and Lee 2021). It also has shown that the bearing factors converge to the exact solution or semi-empirical solutions as aspect ratios increase, with around 7% differences which are not unnoticeable. Secondly, the agreement from the back-analysis of previous FE studies for similar cases is encouraging (Zhang et al. 2011). Thirdly, the FE computations have shown the convergence value as very fine meshes are selected. Despite the above reasons, the accuracy of the 3-D FE predictions remains as a future research demand for reliable estimates, i.e., the influence of stress concentration near the thin caisson or attached parts between the wings and the cylinder (Figure 4). Preliminary 3-D FE studies on the impacts of thicker thickness and adhesion on the axial capacity, i.e., $t_{ring} = t_{wing} = D/20$ and α=0.4, 0.7, and 1, were about 7% greater than the semi-empirical solution. These results may be a possible explanation for the accuracy trend with varying thickness that the stress concentration near the thin caisson may be related to the thickness of the caisson.

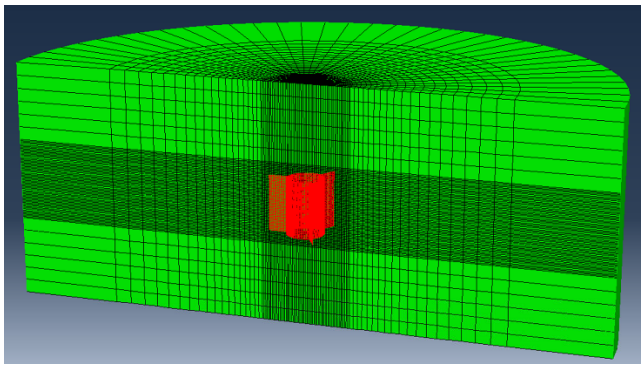

Figure 3. 3-D FE mesh for 3-wings MRA

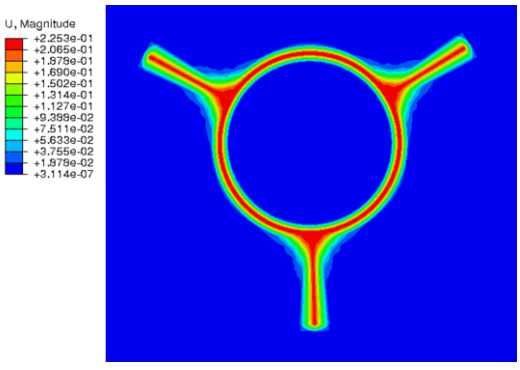

Figure 4. Plan view of 3-D FE results: vertical displacement of 3-wings MRA

PARAMETRIC STUDY

To understand how wing plates enhance the vertical load capacity, this study evaluates the effects of the following parameters.

- The wing plate parameter, $N_w W_w/R$
- Adhesion factor between pile and soil, α

Due to minimizing the required equipment for deepwater installation and mitigating environmental issues, suction installation is often an attractive alternative in soft clays. This leads to the MRA design having the thinner thickness of each component for better installation efficiency. Preliminary findings from semi-empirical solutions indicate that the sensitivity of wing thickness to uplift resistance of the anchor drastically reduces with increasing thickness ratio D/t. This motivates estimating the effects of the adhesion factor on frictional resistance. For these reasons, the current study selects the small thickness for each component, $t_{ring} = t_{wing} = D/100$, to minimize the impact of wing thickness on the vertical capacity.

The axial bearing factor of the MRA with wing plates. The effects of wing plates can be best illustrated through comparison to an axial bearing factor of the cylindrical core. In the case of cylinder-wing plate geometry, different definitions are possible for the axial bearing factor $N_a = V/s_u A$, where V is the ultimate vertical load, s_u is the undrained shear strength of the soil, and A is the selected characteristic dimension of an anchor. Aubeny et al. (2003) selected $A = A_{pc} = DL$, where A_{pc} is the projected area along the side of the cylinder. Bang et al. (2006) took $A = A_{pp} = BL$, where A_{pp} is the projected area of cylinder-wings system normal to the horizontal direction and B is the projected width of the cylinder-wing plates system. This study adopts $A = A_{pc}$ for several reasons. Firstly, this bearing factor definition provides a clear picture of how the wing plates improve the axial capacity compared to that of a simple ring anchor. Secondly, this approach has the advantage of direct comparison to existing solutions for the cylindrical-shaped pile. Thus, a non-dimensional axial bearing factor of the anchor can be defined as follows:

$$N_{ac} = \frac{V}{s_u A_{pc}} = \frac{V}{s_u DL} \tag{1}$$

where V is the ultimate vertical load, s_u is the undrained shear strength of the soil, and A_{pc} is the projected area along the side of the cylinder.

As mentioned earlier, for a fixed suite of selected dimensions of the MRA, in this study L/D =1.5, D/t = 100, and W_w/R = 1, N_{ac} from the empirical approach can be rewritten as simplified forms below in terms of each parameter. The following definitions benefit from getting a clear picture of the sensitivity of each parameter to the axial bearing factor. Both definitions display the linearly increasing trend with increasing each parameter (Table 2).

$$N_{ac} = (2\pi + 1.01N_w)(\alpha) + (0.38 + N_w/20) \tag{2}$$

$$N_{ac} = (1.01\alpha + 0.05)\left(\frac{N_w W_w}{R}\right) + (2\pi\alpha + 0.38) \tag{3}$$

Effect of adhesion factor. As the adhesion factor decreases, illustrated in Figure 5, the axial bearing factor N_{ac} of the MRA decreases up to 50%. A more pronounced decreasing trend of N_{ac} occurs for the cases the MRA has more wing plates. To a great extent, a decrease in frictional resistance along the side of the cylinder and wing plates is a direct consequence of reducing the adhesion factor. The curve fit of each case shows that N_{ac} increases linearly with increasing α. The increasing trend is represented in the gradient of the curve fit, which has shown a similar slope for each case compared to a semi-empirical solution (Table 2). In comparing the cases of no-wing and $N_w = 6$, the sensitivity of the 6-wings MRA capacity to variation in adhesion factor nearly doubles to that of no-wing MRA (i.e., the slope of the no-wing MRA = 6.55 and the slope of the 6-wings MRA = 13.28).

Effect of wing plate parameter. The increase of wing plate parameter N_wW_w/R increases the axial bearing factor N_{ac} of the MRA by nearly 100% (Figure 6). Since the current study considers the MRA that having a thin thickness ratio, the uplift resistance of the MRA is mostly proportional to the side surface area. As indicated in Table 2, y-interception values of the curve fit equations are constant and are the axial bearing factor of the no-wing MRA case under varying adhesion conditions. On the other hand, the variables linearly differ depending on N_wW_w/R and α. In $N_wW_w/R = 6$, N_{ac} has nearly double values compared to that of the MRA without wing plates. This implies that adding wing plates or increasing the width of wing plates is an effective means to improve the vertical load capacity of the MRA.

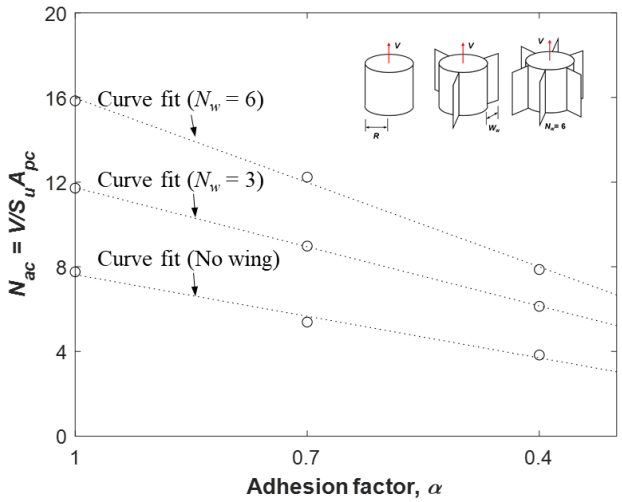

Figure 5. Effect of the adhesion factor, α

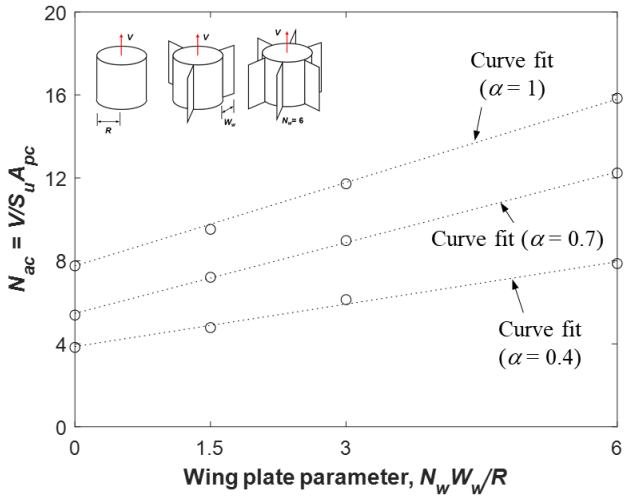

Figure 6. Effect of the wing plate parameter, N_wW_w/R

Table 2. Equations of curve fit

Relationship	Conditions	Curve fit equations		Ref. Figure
		3-D FE	Semi-empirical solution	
N_{ac}-α	$N_w = 6$	$N_{ac} = 13.28(\alpha) + 2.69$	$N_{ac} = 12.34(\alpha) + 0.68$	Figure 5
	$N_w = 3$	$N_{ac} = 9.31(\alpha) + 2.43$	$N_{ac} = 9.31(\alpha) + 0.53$	
	$N_w = 0$	$N_{ac} = 6.55(\alpha) + 1.08$	$N_{ac} = 6.28(\alpha) + 0.38$	
N_{ac}-$N_w W_w/R$	$\alpha = 1$	$N_{ac} = 1.36(N_w W_w/R) + 7.64$	$N_{ac} = 1.06(N_w W_w/R) + 6.67$	Figure 6
	$\alpha = 0.7$	$N_{ac} = 1.14(N_w W_w/R) + 5.47$	$N_{ac} = 0.76(N_w W_w/R) + 4.78$	
	$\alpha = 0.4$	$N_{ac} = 0.68(N_w W_w/R) + 3.87$	$N_{ac} = 0.45(N_w W_w/R) + 2.89$	

OPTIMAL DESIGN OF WING PLATES

As discussed earlier, increasing surface area as much as possible is an effective means to improve load capacity. Different approaches were possible for increasing surface area, such as increasing diameter, adding wing plates, and attaching stiffeners. Since this study focuses on the effects of wing plates on the uplift resistance of the MRA, the comparative study for the cases of the larger diameter without wing plates and smaller diameter with wing plates can be instructive in deciding the best approach to improve vertical load capacity. This study assumes two base cases installed in the same depth and have the same uplift resistance and the same length. Thus, the dimensions of the two base cases have little or no effect on material and fabrication costs. However, the wing plates can provide significant benefits in reducing transport and installation costs due to the ability of the compacted size of the MRA. The cost quantification assumed that transport and installation costs are dependent on anchor dimension. To be precise, the transport costs are proportional to the total trips (= the total required anchor footprints/load per trip) of anchor handling vessels (AHVs). And the installation costs are proportional to suction installation time that is a direct consequence of the interior volume of the tube (Lee et al. 2020). Figures 7-8 and Table 3 indicate that attaching wing plates can be a more economical solution with the comparable capacity to the large diameter without wing plates.

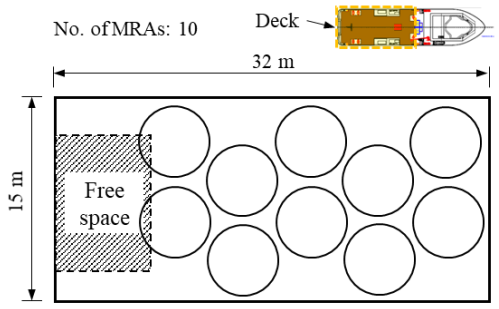

Figure 7. Loading diagram for the larger diameter without wing plates

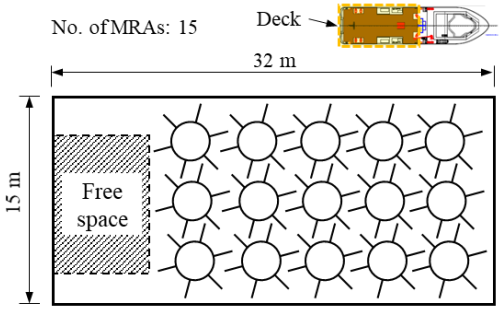

Figure 8. Loading diagram for the smaller diameter with 6 wing plates

Table 3. Comparative study for the optimal design of wing plates

Cases	Uplift resistance[1)]	Anchor dimensions		Interior volume of the tube[2)]	Installation time/anchor[3)]	Load/trip of an AHV[4)]
		Tube	Wing plates			
Larger diameter without wing plates	111 kN	D = 5.2 m, L = 4.2 m	No wing	89.2 m^3 (followers: 267.6 m^3)	6.5 hours	10 anchors (Figure 7)
Smaller diameter with wing plates	110 kN	D = 2.8 m, L = 4.2 m	N_w = 6, $L_w = L$ W_w = 1.4 m (N_wW_w/R = 6)	25.9 m^3 (followers: 77.6 m^3)	1.9 hours	15 anchors (Figure 8)

Assumptions: [1)] uniform undrained shear strength (s_u = 1kPa) and typical adhesion factor (α = 0.7); [2)] tip embedment depth is assumed as h/D = 6 based on the smaller diameter, and the followers for suction installation have the same diameter as the tube. [3)] typical pump capacity for suction installation = 55m^3/hour (Aubeny 2017); [4)] medium size of AHV, deck area = width 15 m by length 32 m = 480 m^2, 15 % of the deck area is for operating space (Ulstein 2020)

CONCLUDING REMARKS

This study presents the potential advantage of wing plates on the MRA to enhance uplift resistance. Three-dimensional FE analyses were conducted to investigate the effects of wing plates on axial load capacity, and it is validated through comparison to the semi-empirical solution. Key findings are as follows:

- Vertical load capacity decreases with decreasing adhesion factor α (Figure 5). This parameter cannot be controlled by the anchor designer; however, considering the typical range of expected α, (0.7-0.9), variation in MRA vertical load capacity can be on the order of 25% due to this parameter.
- Vertical load capacity increase as wing plate parameter N_wW_w/R increases (Figure 6). The use of 6 wing plates of width equal to the cylinder radius can nearly double vertical load capacity.
- Attaching wing plates on the cylinder or increasing the width of the wing plates can be more cost-effective means to enhance the vertical load capacity, since an anchor with wing plates can provide the same vertical load capacity while requiring much less deck space on a transport vessel.

REFERENCES

Andersen, K. H., Murff, J. D., Randolph, M. F., Clukey, E. C., Erbrich, C. T., Jostad, H. P., and Supachawarote, C. (2005). "Suction anchors for deepwater applications." *Proc., INT Symp. On Frontiers in offshore Geotechniques (ISFOG)*. Keynote Lecture, Perth, Australlia, 3-30.

Aubeny, C. (2017). *Geomechanics of Marine Anchors*, CRC Press, Taylor & Francis Group, Boca Raton, FL.

Aubeny, C. P., Han, S. W., and Murff, J. D. (2003). "Inclined load capacity of suction caissons." *International Journal for Numerical and Analytical Methods in Geomechanics*, 27(14), 1235-1254.

Aubeny, C. P., Diaz, B. D., Arwade, S. R., Degroot, D. J., Landon, M. E., Fontana, C., & Hollowell, S. T. (2020). *Multiline Ring Anchor and installation method* (U.S. Patent Application No. 16/978,760) U.S. Patent and Trademark Office.

Aubeny, C. P., and Lee, J. (2021). "Horizontal Load Capacity of Multiline Ring Anchor in Soft Clay." *Proc., International Symposium on Frontiers in Offshore Geotechnics (ISFOG)*, Austin, TX, USA.

Bang, S., Jones, K., Kim, Y. S., Kim, K. O., & Cho, Y. (2006). "Vertical pullout capacity of embedded suction anchors in sand." *The 16th International Offshore and Polar Engineering Conference*, ISOPE, San Francisco, CA, USA, 469-474.

Barter, G. E., Robertson, A., and Musial, W. (2020). "A systems engineering vision for floating offshore wind cost optimization." *Renewable Energy Focus*, 34, 1-16.

Chen, W.-F. (1975). *Limit analysis and soil plasticity*, Elsevier.

Diaz, B. D., Rasulo, M., Aubeny, C. P., Fontana, C. M., Arwade, S. R., DeGroot, D. J., and Landon, M. (2016). "Multiline anchors for floating offshore wind towers." *Proc., OCEANS 2016 MTS/IEEE Monterey*, IEEE, 1-9.

Harries, T., and Grace, A. (2015). Floating wind: buoyant progress. Bloomberg New Energy Finance-Wind research note.

IEA (2019), *Offshore Wind Outlook 2019*, IEA, Paris.

Lee, J., and Aubeny, C. P. (2020). "Multiline Ring Anchor system for floating offshore wind turbines." *Journal of Physics: Conference Series*, 1452, 012036.

Lee, J., Khan, M., Bello, L., and Aubeny, C. P. (2020). "Cost analysis of multiline ring anchor systems for offshore wind farm." *Proc., Deep Foundation Institute 45th Conference*, National Harbor, MD, USA, online, 484-493.

Lee, J., and Aubeny, C. P. (2021). "Effect of keying flaps on a multiline ring anchor in soft clay." *Proc., International Foundation Congress & Equipment Expo*, Dallas, TX, USA, 249-256.

Lee, J., and Aubeny, C. P. (2021). "Lateral undrained capacity of a multiline ring anchor in clay." *International Journal of Geomechanics*, DOI 10.1061/(ASCE)GM.1943-5622.0001995.

Lee, J., Balakrishnan, K., Aubeny, C. P., Arwade, S., DeGroot, D., Martinez, A., and Beemer, R. (2021). "Uplift resistance of a multiline ring anchor system in soft clay to extreme conditions." *Proc., Geo-Extreme Conference*, Savannah, GA, USA, In press.

Murff, J., Randolph, M., Elkhatib, S., Kolk, H., Ruinen, R., Strom, P., and Thorne, C. (2005). "Vertically loaded plate anchors for deepwater applications." *Proc., Proc Int Symp on Frontiers in Offshore Geotechnics*, 31-48.

Musial, W., Heimiller, D., Beiter, P., Scott, G., and Draxl, C. (2016). "*2016 Offshore Wind Energy Resource Assessment for the United States*." National Renewable Energy Lab, Golden, CO, USA.

Randolph, M. F., and Houlsby, G. (1984). "The limiting pressure on a circular pile loaded laterally in cohesive soil." *Geotechnique*, 34(4), 613-623.

Ulstein (2020). "Anchor handling tug supply." <https://ulstein.com/ship-design/ahts>. (March. 27, 2020).

Zhang, Y., Bienen, B., Cassidy, M. J., and Gourvenec, S. (2011). "Undrained bearing capacity of deeply buried flat circular footings under general loading." *Journal of Geotechnical and Geoenvironmental Engineering*, 138(3), 385-397.